Effect of block length on the properties of multiblock polysulfone-poly(diallylpiperidinium hydroxide) anion exchange membranes

Journal:	*Macromolecules*
Manuscript ID	ma-2023-002575.R1
Manuscript Type:	Article
Date Submitted by the Author:	14-May-2023
Complete List of Authors:	Strasser, Derek; Giner Inc Biery, Alison; Colorado School of Mines Department of Chemistry, Chemistry Motz, Andrew; NEL Hydrogen, Seifert, Soenke; Argonne National Laboratory, Chemistry Division Herring, Andrew; Colorado School of Mines, Chemical and Biological Engineering Knauss, Daniel; Colorado School of Mines, Chemistry Department

Effect of block length on the properties of multiblock polysulfone-poly(diallylpiperidinium hydroxide) anion exchange membranes

Derek J. Strasser,[1] Alison R. Biery,[1] Andrew R. Motz,[2] Soenke Seifert,[3] Andrew M. Herring,[2]

*Daniel M. Knauss[1]**

[1]Department of Chemistry and [2]Department of Chemical and Biological Engineering, Colorado School of Mines, Golden CO 80401

[3]X-ray Science Division, Argonne National Laboratory, Argonne, Illinois 60439, United States

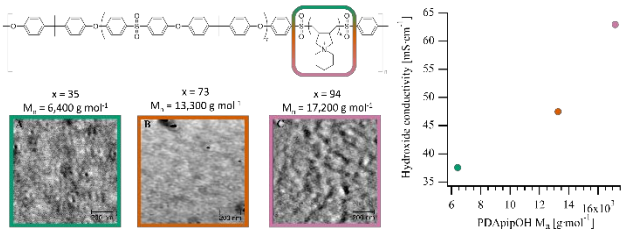

For table of contents use only

ABSTRACT Research in anion exchange membranes (AEM)s has continued with the development of materials bearing base stable cations. Designing AEMs that microphase separate into hydroxide conductive, hydrophilic domains within a hydrophobic and mechanically robust matrix has been shown to be successful for improving AEM performance. A series of multiblock polysulfone-poly(diallylpiperidinium hydroxide) copolymers (PSf-PDApipOH) of similar hydrophobic/hydrophilic composition were prepared in which the molecular weight of the hydroxide conducting PDApipOH segments was varied. The variable hydrophilic segment molecular weight was designed to assess the impact on microphase separation, hydroxide conductivity, and water management. The multiblock copolymers investigated were prepared by condensation polymerization of preformed 4-fluorophenyl sulfone terminated poly(diallylpiperidinium hexafluorophosphate) (PDApipPF6) oligomers with polysulfone monomers. The structure-property relationship between the molecular weight of the conductive PDApipOH segments and AEM performance was demonstrated by evaluation of the microphase separation, water uptake, and hydroxide conductivity. Membranes fabricated from the polysulfone-poly(diallylpiperidinium hexafluorophosphate) (PSf-PDApipPF6) multiblock copolymers were shown to form well-connected conductive domains by SAXS and atomic force

microscopy experiments. The PSf-PDApipOH membranes were highly conductive with the maximum hydroxide conductivity reaching 62.9 mS·cm-1 at 60 ˚C and 95 % relative humidity. Furthermore, it was demonstrated that the conductivity increased with increasing PDApipOH segment molecular weight.

INTRODUCTION

Over the past decade, the electricity produced in the United States by renewable energy sources including wind and solar increased to 20% and coupled with technological and manufacturing advances renewable energy is now cost competitive with legacy fossil fuel electricity generation.[1] The increased deployment and reduced cost of renewable energy has significantly increased interest in hydrogen as a clean energy source and industrial feed stock within the global effort to decarbonize energy sectors. The increased interest in hydrogen technology has rapidly increased research efforts for the development of hydrogen electrochemical devices including alkaline exchange membrane (AEM) electrolyzers and fuel cells.

Research conducted in the last few years in the area of AEM development for alkaline fuel cells has produced exciting membrane materials with improved alkaline stability.[2–8] The advances made in cation stability are enabling new materials to be investigated for AEMs and, with their associated hydroxide conductivities, supporting AEM electrochemical devices as alternatives to commercialized proton exchange membranes. AEMs for use in electrochemical devices including alkaline fuel cells have significant advantages over proton exchange membranes because they have potential to utilize platinum group metal (PGM) free catalysts, and the oxidation-reduction reaction kinetics are faster at high pH conditions.[9–12] However, device performance and operational lifetime are dependent on the ionic conductivity and chemical durability of the membrane material.

Development of microphase separated AEMs in which hydrophilic hydroxide conductive domains form within a hydrophobic and mechanically robust matrix has been shown to be a successful strategy for improving AEM performance.[13] Research conducted on phase-separated materials for AEMs has produced hydrophobic-hydrophilic copolymers of different architectures including block,[14,15,24–29,16–23] graft,[30–38] and comb.[39–41] The resulting AEMs display nanoscale morphological features ranging from spheres to lamellae. It has been shown that AEMs forming

hydrophilic conductive domains have higher conductivity compared to random copolymers of similar structure and composition.[42,43] Furthermore, microphase-separated AEMs have enhanced water management characteristics, resulting in improved swelling behavior.[44–46]

Multiblock is another type of copolymer architecture that has been shown to produce phase-separated membranes.[47,48,57–61,49–56] An advantage of designing multiblock hydrophilic-hydrophobic copolymers is that high molecular weight copolymers can be prepared from a range of molecular weights in the component materials. Research conducted on multiblock polysulfone (PSf) materials has produced copolymers from a variety of bisphenol monomers.[62–66] Manipulation of the multiblock composition and the molecular weight of the component segments can tune the microphase separation.[13] Additionally, multiblock PSf copolymers have been produced with a large range in ion exchange capacities (IECs) and composition of hydrophobic-hydrophilic segments. Due to the good properties of PSf and its incorporation into charged block copolymers, PSf-based membranes are of ongoing interest in ion exchange and fuel cell applications.[43,67] It is therefore important to understand the properties of these materials. However, there are only a few investigations of the structure-property relationships between the component molecular weight at a constant IEC and the multiblock AEM performance.[62,63,68–71]

Poly(diallylpiperidinium hydroxide) (PDApipOH) has been demonstrated to be an exceptionally base stable cationic polymer.[4,5,7] Initial evaluation of PDApipOH incorporated into crosslinked poly(phenylene oxide) membranes indicated high hydroxide conductivity with high water uptake.[5] We have recently demonstrated the first example of hydrophobic-hydrophilic PSf-PDApipOH block copolymers.[4] The PSf-PDApipOH multiblock copolymers display properties of high ionic conductivity along with relatively low water uptake in addition to their base stability. Initial studies of the PSf-PDApipOH membranes in model fuel cells demonstrated reasonable peak power densities and durability.[7]

In the current work, we have designed a series of multiblock PSf-PDApipOH copolymers of similar IEC (Figure 1) in which the molecular weight of the hydrophilic hydroxide conducting PDApipOH segments was varied to assess the impact on AEM performance. Employing the previously established synthetic methods,[4] α,ω-4-fluorophenyl sulfone terminated PDApipPF_6 oligomers were prepared with different molecular weights and subsequently copolymerized with PSf monomers to generate PSf-PDApipPF_6 multiblock copolymers. The solution processable PSf-PDApipPF6 multiblock copolymers were then drop cast to produce AEMs. Ion exchange of the PF_6 counterion was then performed to produce PSf-PDApipOH membranes. The hydrophilic

PDApipOH segments were selected to serve as the conductive phase of the AEM materials owing to their previously established conductivity, chemical and thermal stability, and the regularity of their compact repeat unit structure. The synthetic design produced different PSf-PDApipOH multiblock copolymers that were similar in composition and IEC but varied in the molecular weight of the PDApipOH segments. Membranes were evaluated for the impact of PDApipOH block molecular weight on their morphological characteristics, water uptake, and hydroxide conductivity.

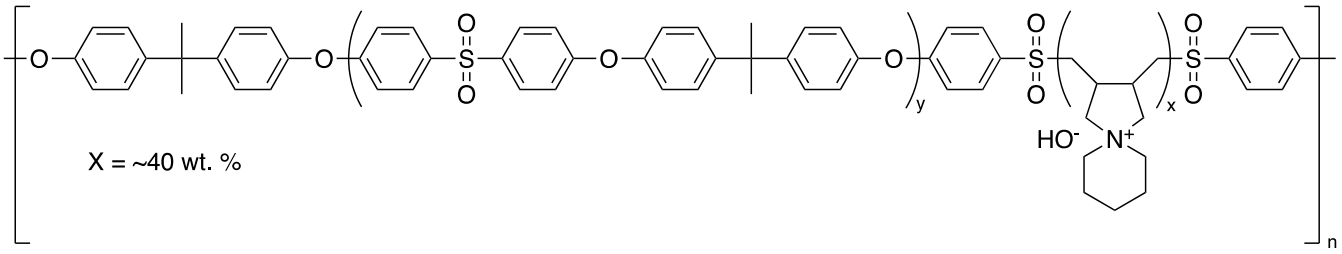

Figure 1. PSf-PDApipOH multiblock copolymer.

EXPERIMENTAL

Materials. Allyl chloride (98%) was purchased from Sigma-Aldrich and was distilled under nitrogen prior to use. *N,N*-dimethylacetamide (DMAc) (99.9%, HPLC grade) was purchased from Sigma-Aldrich and distilled from phosphorous pentoxide. Bisphenol A (97%) and bis(4-fluorophenyl) sulfone (99%) were purchased from Sigma-Aldrich and crystallized twice from

toluene. Piperidine (99%), allyl bromide (99%), 4-fluorothiophenol (98%), and potassium peroxymonosulfate (Oxone) were obtained from Sigma-Aldrich and were used as received. Acetonitrile-d_3, DMSO-d_6, and deuterium oxide were purchased from Sigma-Aldrich. All other chemicals and solvents were used as received from commercial sources.

Synthesis. Synthesis of the photoiniferter bis(4-fluorophenyl) disulfide (BFPDS), monomer *N,N*-diallylpiperidinium chloride, and α,ω-4-fluorophenyl sulfone terminated PDApipPF_6 oligomers were prepared as previously reported.[4] The variation in molecular weight of the α,ω-4-fluorophenyl sulfone terminated PDApipPF_6 oligomers was accomplished by changing the ratio of BFPDS to *N,N*-diallylpiperidinium chloride as follows: A 25 mL stock solution of 2.5 M *N,N*-diallylpiperidinium chloride in water:methanol (3:1) was prepared in a volumetric flask. 10 mL test tubes containing a magnetic stir bar were charged with 40.7 mg (0.16 mmol), 50.8 mg (0.20 mmol), or 68.7 mg (0.27 mmol) BFPDS photoiniferter and 8 mL (20 mmol) of the stock *N,N*-diallylpiperidinium chloride solution. The molar ratio of BFPDS to *N,N*-diallylpiperidinium chloride for each polymerization was calculated to be 1:75, 1:100, and 1:125. The test tubes were sealed with a rubber septum, cooled in an ice bath, and purged with N_2 gas for 20 min. Once purged, the test tubes were placed into a 60 ˚C oil bath, stirred for 20 min and then exposed to

constant UV light (254 nm) while stirring for 24 hours. The 4-fluorophenyl sulfide terminated PDApipCl oligomers were isolated by precipitation into acetone, redissolving the obtained solid mass in methanol (~10 % wt./vol.) and precipitating again into acetone. The 4-flurophenyl sulfide terminated PDApipCl oligomers were collected by vacuum filtration and dried overnight at 80 ˚C under vacuum. The end group oxidation to 4-fluorophenyl sulfone, and ion exchange to hexafluorophosphate were completed as previously described.[4]

Synthesis of multiblock PSf-PDApipPF_6 copolymers. The synthesis of PSf-PDApipPF_6 multiblock copolymers was designed to achieve maximum molecular weight while targeting an IEC of ~ 2.0 in the hydroxide form. To generate the desired multiblock copolymer composition from preformed PDApipPF_6 oligomers, the weight percent of PSf required was calculated in terms of equivalents of bis(4-fluorophenyl) sulfone with respect to the degree of polymerization of the PDApipPF_6 oligomers. The amount of bisphenol A was calculated to give a 1:1 stoichiometric ratio of 4-fluorophenyl and phenoxide reactive species. A representative procedure (PSf-PDApip$PF_6$1) is as follows: a 25 mL 3-neck round bottom flask fitted with an overhead stir motor, Dean-Stark trap prefilled with toluene, condenser, and a N_2 inlet was charged with bisphenol A (0.575 g, 2.52 mmol) and potassium carbonate (0.418 g, 3.02 mmol).

The solids were dissolved in DMAc (10.8 mL) with toluene (3 mL) added to azeotropically remove water. The reaction mixture, under a N_2 atmosphere, was then heated in a 150 ˚C oil bath for 3 hours and then cooled to room temperature. 4-fluorophenyl sulfone terminated PDApip$PF_6$1 (1.50 g, 0.066 mmol) and bis(4-fluorophenyl) sulfone (0.624 g, 2.45 mmol), were then added to the reaction mixture. The solution was heated in a 160 ˚C oil bath overnight, after which time the solution viscosity increased significantly. The viscous solution was diluted with DMAc (10 mL), cooled to room temperature, and precipitated into 200 mL of methanol. The off-white fibers were collected by filtration and boiled in water for 30 minutes to remove residual salts. The polymer fibers were then collected by filtration, and dried in a vacuum oven at 80 ˚C to a constant mass (2.35g, 93 % yield).

Membrane fabrication. PSf-PDApipPF_6 membranes were generated by solution casting the multiblock copolymers in the hexafluorophosphate form. Multiblock PSf-PDApipPF_6 copolymers were dissolved in DMAc to generate a 15 % w/v solution and were deposited onto a glass substrate. The glass was then heated to 75 ˚C and allowed to dry overnight. The PSf-PDApipPF_6 membrane was removed from the glass substrate by submersion in water. The final PSf-PDApipPF_6 membrane was then dried under vacuum overnight.

Ion exchange to hydroxide. The PSf-PDApipPF$_6$ membranes were first exchanged to the bromide form and then to hydroxide. Ion exchange from hexafluorophosphate to bromide was accomplished by submerging the PSf-PDApipPF$_6$ membranes in a saturated aqueous solution of ammonium bromide and soaking at room temperature for 72 hours. Following ion exchange to bromide, the polysulfone-poly(diallylpiperidinium bromide) (PSf-PDApipBr) membranes were then washed twice with deionized water to remove excess ammonium bromide. Soaking the PSf-PDApipBr multiblock copolymer membranes in 1 M KOH for 48 hours completed ion exchange to hydroxide. The final PSf-PDApipOH membranes were then soaked in N_2 purged 18 MΩ water until the washings were neutral pH.

Characterization

NMR Spectroscopy. ^{1}H NMR spectroscopy was performed using a JEOL ECA-500 spectrometer. Chemical shift values (δ) were referenced from residual solvent signals associated with acetonitrile-d$_4$ or DMSO-d$_6$. Average degree of polymerization (DP) values were determined by integrating peaks associated with end groups relative to integrated peaks from backbone protons over multiple spectra and taking the average value.

Atomic Force Microscopy. Tapping mode atomic force microscopy (TM-AFM) was used to elucidate PSf-PDApipBr membrane surface morphology. The phase images were obtained with an Oxford Instruments AFM 3D utilizing a 42 $N \cdot m^{-1}$ Pointprobe AFM tip from Nanoworld. PSf-PDApipBr membranes were cut into 1 cm^2 membranes and adhered to glass microscope slides with double sided tape. The membranes were then heated to 60 ˚C at 95 % RH for 1 hour and subsequently dried under vacuum at room temperature for 24 hours. The images were collected with a driving amplitude of 1 V and the amplitude set point ratio of 0.50 under ambient temperature and humidity.

Small angle X-ray scattering (SAXS). Synchrotron small-angle X-ray scattering experiments were performed at the Advanced Photon Source, Argonne National Laboratories. Experiments were conducted at sector 12-ID-B with the X-ray energy was fixed at 13.3 keV. Using a custom built environmental chamber and previously established measurement techniques,[72,73] scattering experiments were conducted at 60 ˚C at both 0 % and 95 % relative humidity. The PSf-PDApipBr membranes were measured in the bromide form and 2D scattering patterns were obtained. The azimuthally integrated 2D scattering experiments were graphically analyzed by plotting the intensity as a function of the scattering vector magnitude, q, where

$$q\ [\text{Å}^{-1}] = \frac{4\pi \sin(\theta)}{\lambda}$$

λ is 1.03 Å and 2θ is the scattering angle. The Bragg domain spacing, d, was calculated from the equation d = 2π/q.

Ion Exchange Capacity (IEC). The ion exchange capacity of the PSf-PDApipOH membranes was determined from the back-titration method.[74] PSf-PDApipBr membranes were ion exchanged from bromide to hydroxide in 1 M KOH. The PSf-PDApipOH membranes were then washed with N_2 purged 18 MΩ water until the washings were at neutral pH. The PSf-PDApipOH membranes were then neutralized in 20 mL of standardized HCl (0.02501 M) for 48 hours and subsequently vacuum dried at 80 ˚C for 48 hours. The dry mass of the membranes was approximately 0.04 g in the chloride form. The IEC for each membrane was determined, in triplicate, by titrating 3 mL samples of the membrane HCl solution with standardized NaOH (0.004690 M) to determine the amount of unreacted HCl. The IEC was calculated from the following equation:

$$IEC\ [mmol{\cdot}g^{-1}] = \frac{HCl_i - HCl_f}{Mass_d}$$

where HCl_i is the millimoles (mmol) of HCl added to neutralize the membrane, HCl_f is the determined mmol of unreacted HCl after 48 hours and $Mass_y$ is the dry mass (g) of the membrane in the chloride form.

Water Uptake. The percent water uptake (WU%) of each PSf-PDApipBr membrane was determined by dynamic vapor sorption (DVS) with a Surface Measurement Systems DVS Advantage at 60 ˚C and 95 % relative humidity (RH). The membranes were converted from the hexafluorophosphate form to the bromide form and dried under vacuum at 80 ˚C for 48 hours. The membranes were then placed in the DVS environmental chamber and were cycled between dry and hydrated conditions at 60 ˚C three times. The soaking time for each step in the measurement was 120 minutes. Following the measurements, the dry masses and the hydrated masses were averaged, and water uptake percent (WU) was calculated from the following equation:

$$WU\ [\%] = \frac{Mass_h - Mass_d}{Mass_d} \times 100$$

where $Mass_h$ and $Mass_d$ are the hydrated and dry masses for the membrane.

Hydroxide Conductivity. The hydroxide conductivity for the PSf-PDApipOH membranes was determined by electrochemical impedance spectroscopy (EIS) using a Biologic VMP3 potentiostat. In-plane conductivity measurements were made using a Teflon 4-point probe cell with platinum electrodes in a TestEquity environmental chamber set to 60 ˚C and 95 % RH. Membranes were prepared by cutting approximately 2 mm wide strips and ion exchanging from bromide to hydroxide. The PSf-PDApipOH membranes were then washed in N_2 purged 18 MΩ water until the washings were neutral pH. The membranes were then quickly loaded into the test cell and placed in the environmental chamber. EIS measurements were made in the frequency range of 100 Hz to 300 kHz. A minimum of 15 loops were obtained for each membrane to allow for equilibration. Nyquist and Bode plots of the obtained data were analyzed to obtain the high frequency resistance intercept, which was taken as the membrane resistance. The hydroxide conductivity was then determined from the following calculation:

$$\sigma\,[S\cdot cm^{-1}] = \frac{d}{W \times T \times R}$$

where d (cm) is the distance between the reference electrodes, W (cm) and T (cm) are the width and thickness of the membrane and R is the measured resistance (Ω). The membrane dimensions were determined in the hydrated state.

RESULTS AND DISCUSSION

The objective of this research was to investigate the influence of hydrophilic segment molecular weight on the performance of multiblock copolymer anion exchange membranes of similar composition. The multiblock copolymers were designed to contain segments composed of aliphatic spirocyclic repeat units of which various molecular weight prepolymers were incorporated in multiblock copolymer preparations. Reports have indicated that the hydroxide conductivity of AEMs is strongly affected by the phase separation and morphology.[43,75,76] We hypothesized that the hydroxide conductivity of multiblock PSf-PDApipOH copolymers would vary depending on the molecular weight of the hydrophilic PDApipOH segments. In this investigation, we designed and synthesized a series of PSf-PDApipOH multiblock copolymer membranes of similar composition and IEC in which the molecular weight of the conductive PDApipOH segments were varied.

Synthesis of 4-fluorophenyl sulfone terminated PDApipPF_6 oligomers. Disulfides have been employed in radical polymerizations to control the molecular weight of the resulting polymer by degradative chain transfer processes (Scheme 1).[77–79] In the present work, our design

was to produce a series of α,ω-4-fluorophenyl sulfone PDApipPF_6 oligomers of varying molecular weight to be subsequently incorporated in a polysulfone synthesis. Polymerization reactions were completed in a 3:1 methanol/water solvent system with monomer:initiator ratios of 75:1, 100:1 and 125:1. Following polymerization, the α,ω–4-fluorophenyl sulfide oligomers were oxidized with Oxone to the 4-fluorophenyl sulfone derivatives and ion exchanged to the PF_6 form. In our previous work, 4-fluorophenyl sulfone terminated PDApipPF_6 oligomers were produced from a single monomer:initiator ratio of 100:1 and the resultant polymers were confirmed to be difunctional by their ability to produce high molecular weight multiblock PSf-PDApipPF_6 copolymers.[4] By extension, using the same polymerization conditions with different monomer:initiator feed ratios, different α,ω-functionalized oligomers should be produced.

Initiation

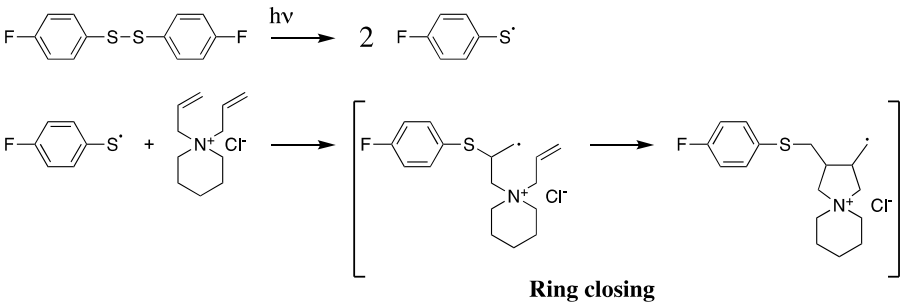

Chain extension

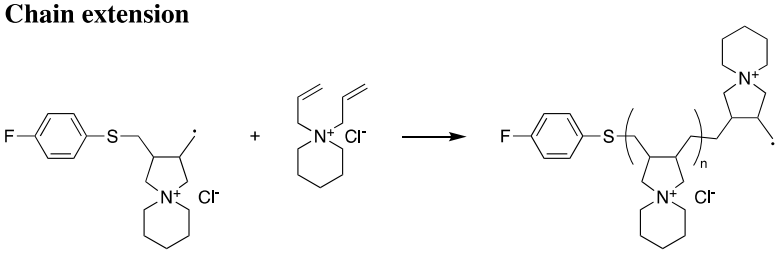

Chain Transfer

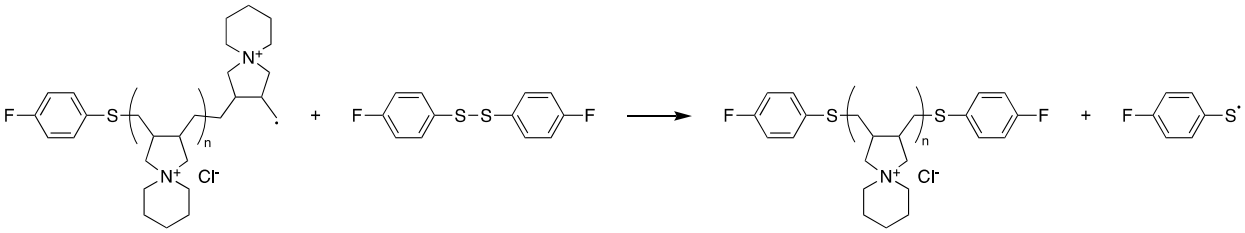

Termination

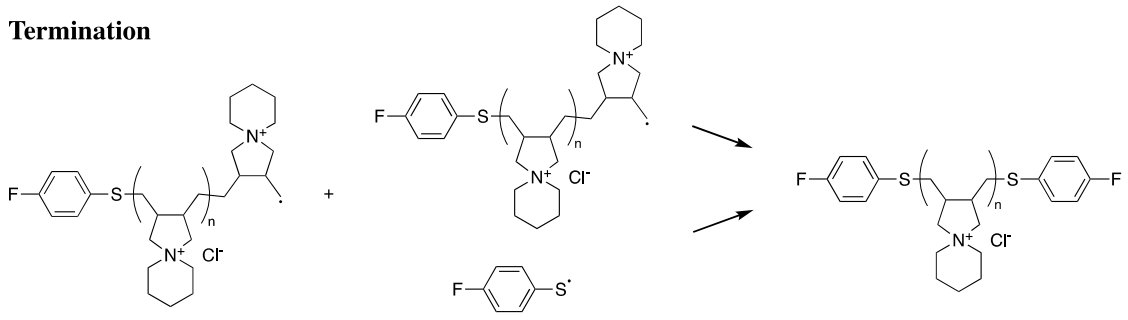

Scheme 1. UV initiated cyclopolymerization of *N,N*-diallylpiperidinium chloride in the presence of BFPDS disulfide photoiniferter.

^{1}H NMR spectroscopy was used to determine the polymer structure and evaluate the number average molecular weight (M_n) of the 4-fluorophenyl sulfone terminated PDApipPF$_6$ oligomers. The ^{1}H NMR spectrum (Figure S1) confirmed the formation of 5-member rings, resulting in spirocyclic repeat units, and the presence of 4-fluorophenyl sulfone end groups. The polymer structure and peak assignment are supported by existing literature investigating the cyclopolymerization of diallylammonium monomers.[4,80,81] Advantageous to determining molecular weight, the 4-fluorophenyl sulfone end groups have spectroscopically unique peaks in the ^{1}H NMR spectra associated with the aromatic ring. The molecular weight of the 4-fluorophenyl sulfone terminated PDApipPF$_6$ oligomers was determined by calculating the degree of polymerization (DP). The DP was obtained by comparing integrals associated with the 4-fluorophenyl sulfone end groups (8 ppm, 4H) and the PDApipPF$_6$ repeat units (3-4 ppm, 2H) for each of the synthesized oligomers (Figure 2). The molecular weights for the 4-fluorophenyl sulfone terminated PDApipPF$_6$ oligomers are reported in Table 1. Additionally, the concentration of 4-fluorophenyl sulfone end groups per known mass of polymer was determined from the ^{1}H NMR spectra. The addition of a known mass of methylene bromide to NMR samples containing a known mass of polymer produced NMR spectra with a spectroscopically

unique standard peak. The mass of 4-fluorphenyl sulfone end groups per mass of polymer was then determined by comparison of the integral values associated with the 4-flurophenyl sulfone end groups and the methylene bromide. It was assumed that determination of the 4-fluorophenyl sulfone end group concentration by directly measuring it from NMR spectroscopy, as described, was more accurate compared to calculating the concentration in a known quantity based on the molecular weight determined from the NMR spectra. The molecular weight determined from NMR spectroscopy assumes that each chain is difunctional therefore the ratio of end groups to repeat units gives the DP and a molecular weight estimation. However, the molecular weight determined by this method would not account for a mixture of counterions so, it was assumed to be a less reliable description of end group concentration. Furthermore, for simplicity the molecular weights presented below are all calculated in the hydroxide form, not only because hydroxide is the counter ion for the application it is also directly measured and supports copolymer composition.

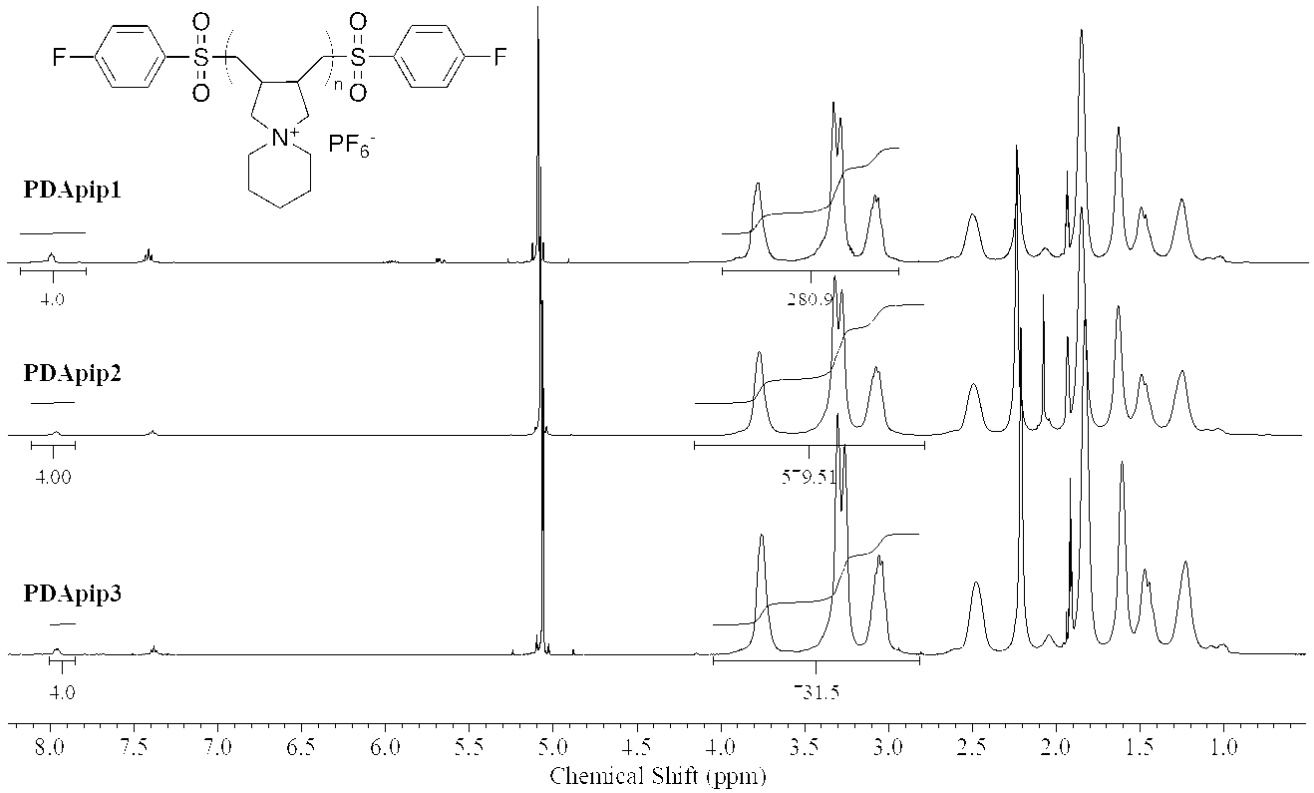

Figure 2. ^{1}H NMR spectra of PDApip prepolymers. The signal at 8 ppm corresponds to the four aromatic protons adjacent to the sulfone and the signals at 3-4 ppm correspond to the 8 protons adjacent to the quaternary ammonium.

Table 1. Molecular weight characterization of PDApip oligomers

Sample	[BFPDS]: [DApip]	DP[a]	M_n [b] [g·mol^{-1}]	Conversio [%]
PDApip1	1:75	35	6,400	22
PDApip2	1:100	73	13,300	37

PDApip3	1:125	94	17,200	27

a) Determined from ^{1}H NMR spectra; b) calculated in the hydroxide form.

PDApipPF_6 oligomers with increasing DP were produced by the UV initiated cyclopolymerization of *N,N*-diallylpiperidinium chloride by increasing the monomer to initiator ratio. The molecular weights of the oligomers were calculated from the DP (Table 1). The molecular weights of the oligomers depend on the identity of the counterion, with different molecular weights for the repeat unit of a given oligomer in the PF_6 (311.25 g·mol^{-1}) versus the hydroxide (183.30 g·mol^{-1}) form. The molecular weights of the oligomers in the PF_6 form were determined to be 10,900, 22,700, and 29,200 g·mol^{-1} for PDApip1, PDApip2, and PDApip3, respectively and 6,400, 13,300 and 17,200 g·mol^{-1} for the three oligomers when calculated in the hydroxide form.

Synthesis of PSf-PDApip multiblock copolymers. Multiblock copolymers were produced by condensation polymerization of the preformed 4-fluorophenyl sulfone functionalized PDApipPF_6 oligomers with the polysulfone monomers, bisphenol A and bis(4-fluorophenyl) sulfone. The objective of the polymerizations was to produce a series of PSf-PDApip multiblock copolymers

with consistent weight fraction of PDApipOH (targeted at 40 wt. %) from the different molecular weight $PDApipPF_6$ starting materials. PSf-PDApip multiblock copolymers with the same weight fraction of PDApipOH regardless of the PDApipOH oligomer molecular weight would have the same IEC and allow for the determination of property differences related to the hydroxide conducting segment molecular weight. The copolymerizations produced materials in yields greater than 90 %. The mole percent of PDApip incorporated into the PSf-PDApip copolymers was calculated from the ^{1}H NMR spectra. Compositions of the PSf-PDApip multiblock copolymers were determined by comparing peak integrals associated with the PSf repeat unit (B, 4H) and the PDApip repeat unit (downfield E, 2H at 3.8 ppm) (Figure 3) (^{1}H NMR spectra for all three samples in Figure S2). It was assumed that the contribution of the PDApip end groups to the B peak associated with the PSf repeat units was negligible. The weight percentage of PDApip in the copolymers was determined by calculation using the molecular weight of the oligomers in the hydroxide form (Table 2).

Table 2. Summary of PSf-PDApipOH multiblock copolymer compositions

Sample	DP[a]	PDApipOH M_n[a] [g·mol^{-1}]	PDApipOH[a] mol.%	PDApipOH[b] wt.%
PSf-PDApip1	35	6,400	58.6	36.9
PSf-PDApip2	73	13,300	61.0	39.3
PSf-PDApip3	94	17,200	59.6	37.9

a) Determined from the ^{1}H NMR spectrum b) Calculated from the mole percent (based on hydroxide

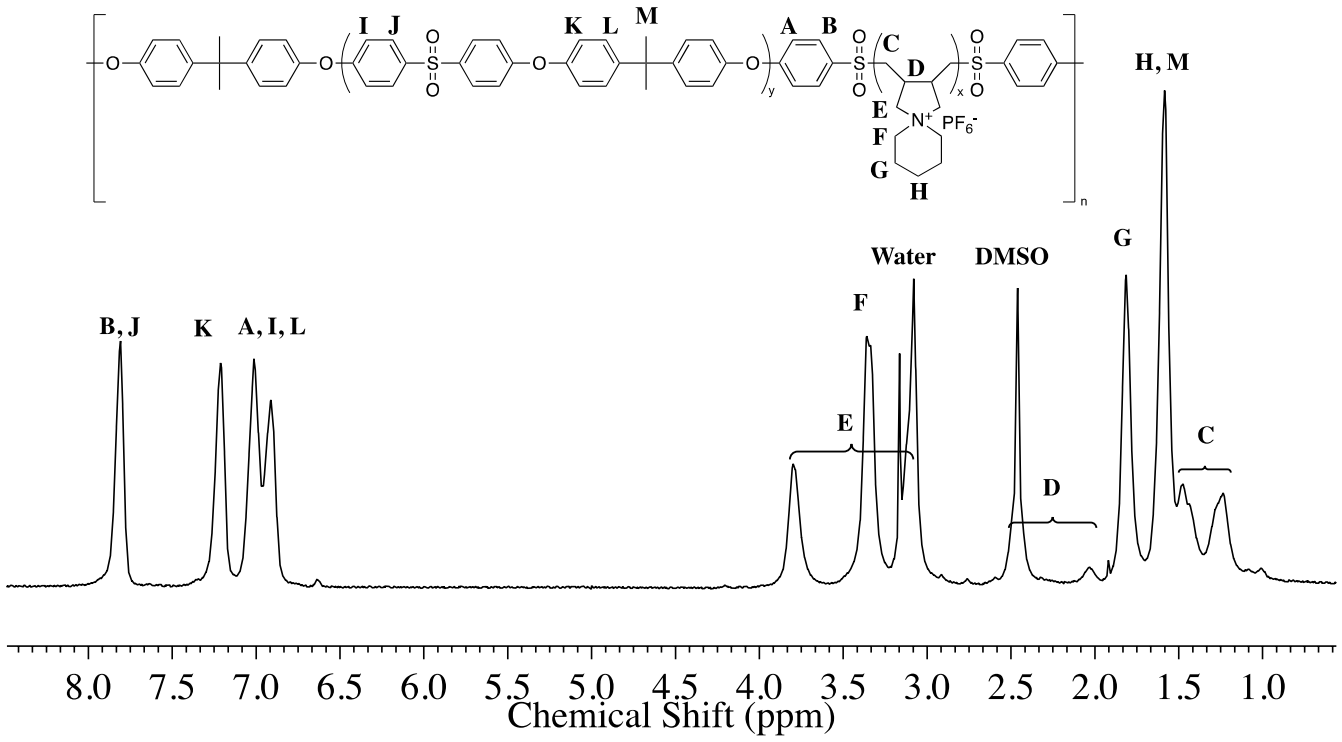

Figure 3. ^{1}H NMR spectrum of PSf-PDApip3.

Membrane formation and ion exchange to hydroxide. The PSf-PDApip multiblock copolymers were fabricated into AEMs by solvent casting followed by ion exchange. The multiblock copolymers were dissolved in DMAc and the solutions were drop cast onto glass slides held at 75 ˚C. The resulting membranes were found to be colorless and transparent. The PSf-PDApipPF_6 multiblock copolymer membranes were ion exchanged to hydroxide following an ion exchange first to bromide. Ion exchange from PF_6 to chloride by heating PSf-PDApipPF_6 membranes in a saturated solution of ammonium chloride at 100 ˚C was reported in our earlier work.[4] In this study, ion exchange to bromide under milder conditions was found to be an effective intermediate step and was completed by soaking the membranes in saturated ammonium bromide at room temperature over 72 hours followed by repeated washings to remove the excess salt. Ion exchange to hydroxide was then accomplished by soaking the PSf-PDApipBr membranes in 1 M KOH and rinsing the membranes with N_2 purged 18 MΩ water.

Physical properties: IEC and water uptake. Back-titration of hydroxide in the PSf-PDApipOH multiblock copolymer membranes was completed to determine the complete removal of PF_6 and to characterize the IEC of each membrane. Removal of PF_6 from the PSf-PDApipPF_6 membranes is important for the accurate characterization of the water uptake and

hydroxide conductivity due to the increased hydrophobic character and bulk of the PF_6 counterion. The membranes were neutralized in a standardized HCl solution. Following neutralization, the remaining acid solutions were titrated five times to obtain the IEC for the membranes (Table 3). The IEC values determined by back-titration of hydroxide are shown to be in close agreement with the IEC values estimated from the composition for the PSf-PDApipOH multiblock copolymers determined by NMR spectroscopy. The slightly lower IECs obtained by titration compared to the values obtained by NMR spectroscopy could be attributed to incomplete ion exchange.

Table 3. Characterization of PSf-PDApip multiblock copolymer membranes.

Membrane	IEC ^{1}H NMR[a] [mmol·g^{-1}]	IEC [HO^-][b] [mmol·g^{-1}]	Water Uptake[c] [wt.%]	σ[c] [mS·cm^{-1}]
PSf-PDApip1	2.02	1.86 ± 0.04	17.0 ± 0.010	37.5 ± 0.3
PSf-PDApip2	2.14	1.99 ± 0.07	21.8 ± 0.015	47.4 ± 0.6
PSf-PDApip3	2.07	1.71 ± 0.07	19.4 ± 0.012	62.9 ± 1.9

a) Determined from the ^{1}H NMR spectrum composition and calculated in the hydroxide form. b) Measured by back-titration of hydroxide. c) Water uptake by DVS in the bromide form measured at 60 ˚C and 95 % RH. d) hydroxide conductivity measured at 60 ˚C and 95 % RH.

Water uptake is an important factor that affects ionic conductivity in AEMs. Evaluation of the water uptake using humidified air rather than liquid water is important for a more accurate assessment of membrane performance in applications that utilize humidified gases e.g., alkaline fuel cells. Water absorbed in AEMs is known to dissociate the cationic groups of the membrane material and facilitate hydroxide transport.[46,48,68,82] Membranes that exhibit higher water uptake tend to have higher hydroxide conductivity compared to membranes with lower water uptake. However, as demonstrated by previous characterization of PSf-PDApipOH membranes in model fuel cells, excessive water uptake can also have the deleterious effects of diluting the cations in the membrane material, which decreases the volumetric IEC and mechanical strength.[7] In this study, the water uptake for the PSf-PDApip membranes was evaluated at 60 ˚C and 95 % relative humidity in the bromide form by dynamic vapor sorption (DVS) (Table 3). The PSf-PDApipBr multiblock copolymer membranes showed low water uptake values of 17.0, 21.8, and 19.4 wt.% for PSf-PDApip1, PSf-PDApip2 and PSf-PDApip3 membranes, respectively. Evaluation of the water uptake was completed in the bromide from to eliminate the effects of carbonate and

bicarbonate formation during the measurements. Minimal variability was observed in the water uptake measurements due to the membranes having similar IECs. However, the slight variation in the composition of the three multiblock copolymer samples resulted in the PSf-PDApip2 membrane demonstrating the highest water uptake, which corresponded with the highest IEC. The modest water uptake values for the PSf-PDApipBr membranes were considered to be a result of the multiblock copolymer phase separation into hydrophobic glassy PSf and hydrophilic domains. The low water uptake values determined by DVS for the hydrophobic-hydrophilic PSf-PDApipBr copolymer membranes are similar to the low water uptake values of other hydrophobic-hydrophilic block copolymer membranes produced in our group.[83]

Hydroxide conductivity. For alkaline fuel cell application, the hydroxide conductivity is of particular interest. Although the effect of the relative piperidinium content on the properties of multiblock polysulfones has been examined,[4,7] studies which specifically investigate the influence of block length on polymer performance are rare. It has been reported that AEMs derived from diblock copolymers of similar compositions with varying hydrophilic block lengths (prepared by controlled-living radical polymerization techniques) show an increase in hydroxide conductivity with increasing hydrophilic block length. This finding was attributed to the

membrane morphology.[84,85] The PSf-PDApipOH multiblock copolymer membranes were evaluated for their hydroxide conductivity at 60 ˚C and 95 % RH. The results of the in-plane EIS experiments (Figure 4) indicate that the hydroxide conductivity was strongly dependent on the segment length of the PDApipOH. While there was some variation in the multiblock copolymer IEC, the variation in IEC and the concomitant water uptake (Table 3) had a minimal impact on the conductivity compared to the segment length of the PDApipOH segments. Illustrating this effect, the PSf-PDApip1 membrane (IEC = 1.86), which was synthesized from PDApip1 (DP = 35; M_n = 6,400 g·mol^{-1}) had a hydroxide conductivity of 37.5 mS·cm^{-1}. In contrast, the PSf-PDApip3 membrane (IEC = 1.76), which was synthesized from PDApip3 (DP= 94; M_n = 17,200 g·mol^{-1}) had a hydroxide conductivity of 62.9 mS·cm^{-1}. These results indicate that the nanoscale, conductive domains in the PSf-PDApip membranes are largely responsible for the membrane performance. With respect to multiblock PSf copolymer AEMs, there are reports in which the composition of materials has been investigated and by extension, membranes with similar composition but different segment molecular weights.[62,63,68–71] Hu et al. produced a series of benzyltrimethyl ammonium functionalized membranes (titrated IEC ~ 1.3) wherein the hydroxide conductivity at 60 ˚C increased from 15.4 to 29.4 mS·cm^{-1} as a result of increasing the

hydrophilic segment molecular weight.[68] However, the phase separation of the membranes was not investigated. In contrast, there are several studies of multiblock PSf copolymer AEMs wherein no discernable trend in the relationship between segment molecular weight and hydroxide conductivity was observed.[62,63,69]

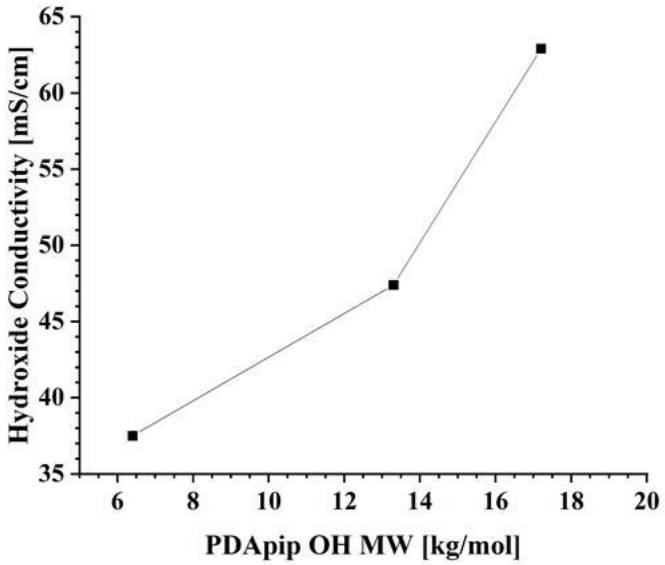

Figure 4. Plot of hydroxide conductivity vs. PDApipOH segment molecular weight.

Membrane phase separation. Developing AEMs with hydrophobic-hydrophilic phase separated morphology is important for the formation of well-connected hydroxide conducting domains. SAXS characterization of AEMs has been employed to determine the Bragg spacing between formed ionic clusters within the phase separated morphology of the bulk material.[48,64] The multiblock copolymer PSf-PDApipBr membranes were investigated by SAXS in order to

characterize the phase separation. The SAXS profiles for the PSf-PDApipBr membranes were obtained at 60 ˚C under both dry and 95 % RH conditions. The scattering peaks exhibited by the PSf-PDApipBr membranes are attributed to the aggregation of PDApipBr segments corresponding to hydrophilic domains and their average spacing. Shown in Figure 5A, the PSf-PDApip2 and PSf-PDApip3 membranes exhibited strong scattering peaks corresponding to domain spacings of 24 and 25 nm, respectively. The PSf-PDApip1 membrane showed a weaker scattering peak corresponding to a smaller domain spacing of 18 nm. The general trend of smaller domain spacing for copolymers with shorter PDAPip segments was expected due to the corresponding lower molecular weight PSf segments in the copolymer. Because of the in-situ multiblock synthesis method used, smaller length PDApip oligomers result in shorter PSf segments, i.e., a greater number of shorter blocks of each component comprise the copolymer. Shorter PDApip oligomers should result in smaller aggregated domains and the shorter PSf blocks should produce a smaller separation of the hydrophilic PDApipBr domains.

When the RH was increased to 95% (Figure 5B), the scattering intensity decreased for all the PSf-PDApipBr membranes. The decrease in the intensity of the scattering peaks with increased humidity indicated that the water uptake disrupted the PDApipBr domains. However, the domain

spacing did not change appreciably with the increase of RH, which indicated that the swelling was minimal and that the membranes exhibit dimensional stability. Lastly, the absence of secondary scattering peaks in the SAXS profiles indicates that the PSf-PDApipBr membranes did not form long-range, well-ordered morphological features.

Domain spacing correlates somewhat with the hydroxide conductivity; however, PSf-PDApip2 and PSf-PDApip3 show similar SAXS profiles, yet significantly different hydroxide conductivity. The possibility of dissolution of differing amounts of one component into the other and how that may be affected by the number of sequence changes and molecular weight of component blocks could have a greater impact on conductivity than the aggregation of the bulk of the ionic component as measured by SAXS.

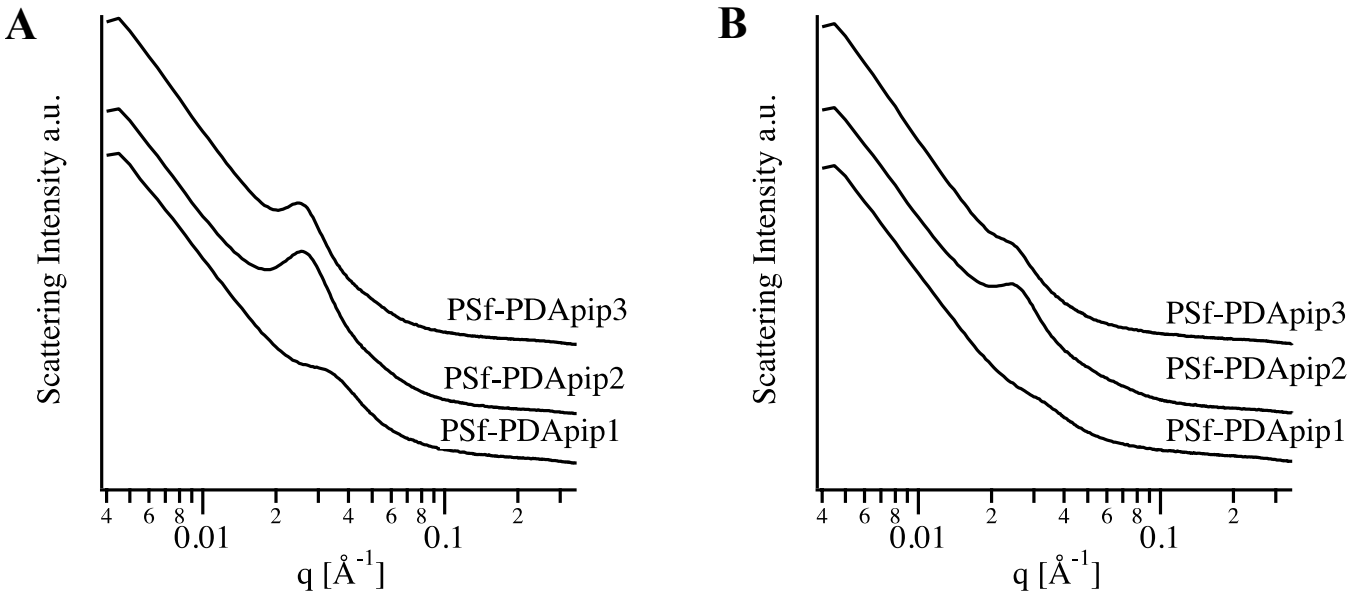

Figure 5. SAXS profile for PSf-PDApipBr membranes at 60 ˚C and 0 % RH (A) and at 60 ˚C and 95 % RH (B).

Phase separation and the corresponding domain spacing for each of the PSf-PDApipBr membranes was indicated by SAXS and demonstrates that while the membranes are comprised of copolymers with similar hydrophilic to hydrophobic content and similar IEC and water uptake, notable differences are observed in the scattering plots. Further investigation of the phase separation was done by TM-AFM on the PSf-PDApipBr membranes to elucidate the surface morphology. Phase images were generated from membranes treated at 60 ˚C and 95 % RH prior to measurement such that membrane phase separation would correlate closely to the SAXS and

hydroxide conductivity measurements. The phase images produced (Figure 6) clearly indicate hydrophobic-hydrophilic phase separation and the absence of well-ordered structures.

While it is difficult to accurately correlate differences in the phase images with the different properties of the membranes, the phase images seem to indicate that increasing molecular weight in the PDApipBr segments improves the connectivity of domains. This is most obvious between PSf-PDApip1 (Figure 6A) and PSf-PDApip3 (Figure 6C) where the darker domains appear to make longer connected paths (it has previously been determined that the dark phases correspond to the cationic polymer segments.[4]) An improved connectivity of hydrophilic conductive pathways in the AFM images would support the increase of the hydroxide conductivity with increasing PDApipOH segment length. It is important to note that the AFM images are examining the surface morphology while the SAXS analysis is attributed to the bulk morphology.

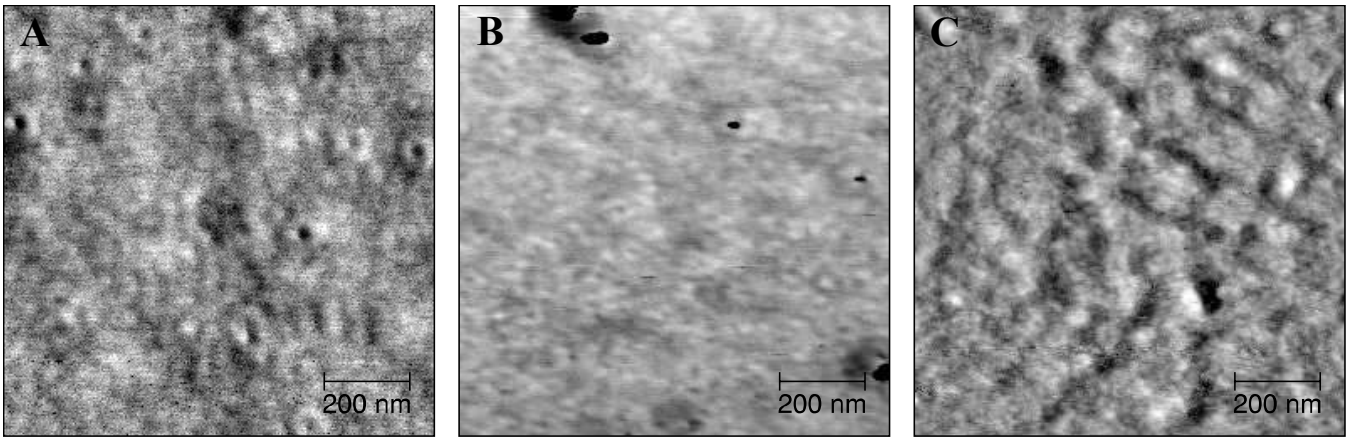

Figure 6. AFM phase images for PSf-PDApip1 (A), PSf-PDApip2 (B), and PSf-PDApip3(C) taken under ambient temperature and humidity.

CONLUSIONS

This study investigated the structure-property relationships between ion conductive segment molecular weight, morphology, and AEM performance for multiblock PSf-PDApipOH copolymer membranes. The work implemented photoinitiated degradative chain transfer cyclopolymerization to produce 4-fluorophenyl sulfone terminated PDApipPF_6 oligomers of different molecular weights. The oligomers were subsequently incorporated into PSf-PDApipPF_6 multiblock copolymers by polycondensation reactions in the presence of PSf monomers. Using the different molecular weight oligomers, the PDApip to PSf composition was maintained to result in copolymers with similar IECs so that the differences in performance could be measured and

attributed to the variation in block length of the PDApip segments. The resulting multiblock PSf-PDApipPF_6 copolymers were fabricated into membranes and after ion exchange to the bromide form, each of the membranes exhibited similar properties of low water uptake under conditions of 95% RH. SAXS and TM-AFM were employed to elucidate the morphology of the copolymer membranes, and it was observed that the membranes with different PDApip segment lengths exhibited different characteristics. Ion exchange to hydroxide and measurement of the hydroxide conductivity showed that increasing PDApipOH segment length, resulted in a significant increase in ionic conductivity and that the ionic conductivity is potentially correlated to the phase morphology. While only a specific set of multiblock PSf-PDApip copolymers were examined, the results are significant in demonstrating that the AEM properties are dependent on factors beyond IEC and composition. PDApip oligomers with larger segment lengths were not evaluated and so it is unknown if the general trend of increasing segment length continues to correlate with a higher ionic conductivity or if the increases in conductivity are due to other factors that may result from the variation of segment length. However, the results encourage further investigation into the structure property relationships of multiblock AEM materials and that block segment length of hydrophilic segments can have a significant impact on the properties.

ACKNOWLEDGEMENTS

This material is based upon work supported by the U.S. Army Research Laboratory and the U.S. Army Research Office under MURI contract/grant number W911NR-10-1-0520. This research used resources of the Advanced Photon Source, a U.S. Department of Energy (DOE), Office of Science, User Facility operated for the DOE Office of Science by Argonne National Laboratory under Contract No. DE-AC02-06CH11357.

AUTHOR INFORMATION

Corresponding Author

* E-mail: dknauss@mines.edu

ORCID

Derek J. Strasser: 0000-0001-6844-4570

Alison R. Biery: 0000-0003-1335-3713

Soenke Seifert: 0000-0003-4598-2354

Andrew M. Herring: 0000-0001-7318-5999

Daniel M. Knauss: 0000-0001-9445-5505

Author Contributions

The manuscript was written through contributions of all authors. All authors have given approval to the final version of the manuscript.

Notes

The authors declare no competing financial interest.

REFERENCES

(1) Cole, W.; Gates, N.; Mai, T. Exploring the Cost Implications of Increased Renewable Energy for the U.S. Power System. *Electr. J.* **2021**, *34* (5), 106957. https://doi.org/10.1016/j.tej.2021.106957.

(2) Dang, H. S.; Jannasch, P. Alkali-Stable and Highly Anion Conducting Poly(Phenylene Oxide)s Carrying Quaternary Piperidinium Cations. *J. Mater. Chem. A* **2016**, *4* (30), 11924–11938. https://doi.org/10.1039/c6ta01905f.

(3) Gu, F.; Dong, H.; Li, Y.; Sun, Z.; Yan, F. Base Stable Pyrrolidinium Cations for Alkaline

Anion Exchange Membrane Applications. *Macromolecules* **2014**, *47* (19), 6740–6747. https://doi.org/10.1021/ma5015148.

(4) Strasser, D. J.; Graziano, B. J.; Knauss, D. M. Base Stable Poly(Diallylpiperidinium Hydroxide) Multiblock Copolymers for Anion Exchange Membranes. *J. Mater. Chem. A* **2017**, *5* (20), 9627–9640. https://doi.org/10.1039/c7ta00905d.

(5) Olsson, J. S.; Pham, T. H.; Jannasch, P. Poly(N,N-Diallylazacycloalkane)s for Anion-Exchange Membranes Functionalized with N-Spirocyclic Quaternary Ammonium Cations. *Macromolecules* **2017**, *50* (7), 2784–2793. https://doi.org/10.1021/acs.macromol.7b00168.

(6) Yang, K.; Ni, H.; Du, X.; Shui, T.; Shen, H.; Xu, J.; Liu, Y.; Li, C.; Gao, Y.; Wang, Z. Improvement the Hydroxide Conductivity and Alkaline Stability Simultaneously of Anion Exchange Membranes by Changing Quaternary Ammonium and Imidazole Contents. *Int. J. Energy Res.* **2021**, *45* (9), 13668–13680. https://doi.org/10.1002/er.6698.

(7) Yang-Neyerlin, A. C.; Medina, S.; Meek, K. M.; Strasser, D. J.; He, C.; Knauss, D. M.; Mustain, W. E.; Pylypenko, S.; Pivovar, B. S. Editors' Choice—Examining Performance and Durability of Anion Exchange Membrane Fuel Cells with Novel Spirocyclic Anion

Exchange Membranes. *J. Electrochem. Soc.* **2021**, *168* (4), 044525. https://doi.org/10.1149/1945-7111/abf77f.

(8) Wang, J.; Zhao, Y.; Setzler, B. P.; Rojas-Carbonell, S.; Ben Yehuda, C.; Amel, A.; Page, M.; Wang, L.; Hu, K.; Shi, L.; et al. Poly(Aryl Piperidinium) Membranes and Ionomers for Hydroxide Exchange Membrane Fuel Cells. *Nat. Energy* **2019**, *4* (5), 392–398. https://doi.org/10.1038/s41560-019-0372-8.

(9) Merle, G.; Wessling, M.; Nijmeijer, K. Anion Exchange Membranes for Alkaline Fuel Cells: A Review. *J. Memb. Sci.* **2011**, *377* (1–2), 1–35. https://doi.org/10.1016/j.memsci.2011.04.043.

(10) Couture, G.; Alaaeddine, A.; Boschet, F.; Ameduri, B. Polymeric Materials as Anion-Exchange Membranes for Alkaline Fuel Cells. *Prog. Polym. Sci.* **2011**, *36* (11), 1521–1557. https://doi.org/10.1016/j.progpolymsci.2011.04.004.

(11) Hren, M.; Božič, M.; Fakin, D.; Kleinschek, K. S.; Gorgieva, S. Alkaline Membrane Fuel Cells: Anion Exchange Membranes and Fuels. *Sustain. Energy Fuels* **2021**, *5* (3), 604–637. https://doi.org/10.1039/d0se01373k.

(12) Das, G.; Choi, J. H.; Nguyen, P. K. T.; Kim, D. J.; Yoon, Y. S. Anion Exchange Membranes for Fuel Cell Application: A Review. *Polymers (Basel).* **2022**, *14* (6). https://doi.org/10.3390/polym14061197.

(13) Li, N.; Guiver, M. D. Ion Transport by Nanochannels in Ion-Containing Aromatic Copolymers. *Macromolecules* **2014**, *47* (7), 2175–2198. https://doi.org/10.1021/ma402254h.

(14) Elabd, Y. A.; Hickner, M. A. Block Copolymers for Fuel Cells. *Macromolecules* **2011**, *44* (1), 1–11. https://doi.org/10.1021/ma101247c.

(15) Kostalik, H. A.; Clark, T. J.; Robertson, N. J.; Mutolo, P. F.; Longo, J. M.; Abruña, H. D.; Coates, G. W. Solvent Processable Tetraalkylammonium-Functionalized Polyethylene for Use as an Alkaline Anion Exchange Membrane. *Macromolecules* **2010**, *43* (17), 7147–7150. https://doi.org/10.1021/ma101172a.

(16) Ma, Y.; Wu, G.; Yang, W. Synthesis and Properties of the Ionomer Diblock Copolymer Poly(4-Vinylbenzyl Triethyl Ammonium Bromide)-b-Polyisobutene. *J. Polym. Sci. Part A Polym. Chem.* **2003**, *41* (18), 2755–2764. https://doi.org/10.1002/pola.10815.

(17) Noonan, K. J. T.; Hugar, K. M.; Kostalik, H. A.; Lobkovsky, E. B.; Abruña, H. D.; Coates, G. W. Phosphonium-Functionalized Polyethylene: A New Class of Base-Stable Alkaline Anion Exchange Membranes. *J. Am. Chem. Soc.* **2012**, *134* (44), 18161–18164. https://doi.org/10.1021/ja307466s.

(18) Rebeck, N. T.; Li, Y.; Knauss, D. M. Poly(Phenylene Oxide) Copolymer Anion Exchange Membranes. *J. Polym. Sci. Part B Polym. Phys.* **2013**, *51* (24), 1770–1778. https://doi.org/10.1002/polb.23245.

(19) Sun, L.; Guo, J.; Zhou, J.; Xu, Q.; Chu, D.; Chen, R. Novel Nanostructured High-Performance Anion Exchange Ionomers for Anion Exchange Membrane Fuel Cells. *J. Power Sources* **2012**, *202*, 70–77. https://doi.org/10.1016/j.jpowsour.2011.11.023.

(20) Tsai, T. H.; Maes, A. M.; Vandiver, M. A.; Versek, C.; Seifert, S.; Tuominen, M.; Liberatore, M. W.; Herring, A. M.; Coughlin, E. B. Synthesis and Structure-Conductivity Relationship of Polystyrene-Block- Poly(Vinyl Benzyl Trimethylammonium) for Alkaline Anion Exchange Membrane Fuel Cells. *J. Polym. Sci. Part B Polym. Phys.* **2013**, *51* (24), 1751–1760. https://doi.org/10.1002/polb.23170.

(21) Vinodh, R.; Ilakkiya, A.; Elamathi, S.; Sangeetha, D. A Novel Anion Exchange Membrane from Polystyrene (Ethylene Butylene) Polystyrene: Synthesis and Characterization. *Mater. Sci. Eng. B Solid-State Mater. Adv. Technol.* **2010**, *167* (1), 43–50. https://doi.org/10.1016/j.mseb.2010.01.025.

(22) Weber, R. L.; Ye, Y.; Schmitt, A. L.; Banik, S. M.; Elabd, Y. A.; Mahanthappa, M. K. Effect of Nanoscale Morphology on the Conductivity of Polymerized Ionic Liquid Block Copolymers. *Macromolecules* **2011**, *44* (14), 5727–5735. https://doi.org/10.1021/ma201067h.

(23) Ye, Y.; Choi, J. H.; Winey, K. I.; Elabd, Y. A. Polymerized Ionic Liquid Block and Random Copolymers: Effect of Weak Microphase Separation on Ion Transport. *Macromolecules* **2012**, *45* (17), 7027–7035. https://doi.org/10.1021/ma301036b.

(24) Ye, Y.; Sharick, S.; Davis, E. M.; Winey, K. I.; Elabd, Y. A. High Hydroxide Conductivity in Polymerized Ionic Liquid Block Copolymers. *ACS Macro Lett.* **2013**, *2* (7), 575–580. https://doi.org/10.1021/mz400210a.

(25) Zeng, Q. H.; Liu, Q. L.; Broadwell, I.; Zhu, A. M.; Xiong, Y.; Tu, X. P. Anion Exchange

Membranes Based on Quaternized Polystyrene-Block-Poly(Ethylene-Ran-Butylene)-Block-Polystyrene for Direct Methanol Alkaline Fuel Cells. *J. Memb. Sci.* **2010**, *349* (1–2), 237–243. https://doi.org/10.1016/j.memsci.2009.11.051.

(26) Li, Y.; Liu, Y.; Savage, A. M.; Beyer, F. L.; Seifert, S.; Herring, A. M.; Knauss, D. M. Polyethylene-Based Block Copolymers for Anion Exchange Membranes. *Macromolecules* **2015**, *48* (18), 6523–6533. https://doi.org/10.1021/acs.macromol.5b01457.

(27) Yang, Y.; Knauss, D. M. Poly(2,6-Dimethyl-1,4-Phenylene Oxide)- b -Poly(Vinylbenzyltrimethylammonium) Diblock Copolymers for Highly Conductive Anion Exchange Membranes. *Macromolecules* **2015**, *48* (13), 4471–4480. https://doi.org/10.1021/acs.macromol.5b00459.

(28) Zhang, K.; Gong, S.; Zhao, B.; Liu, Y.; Qaisrani, N. A.; Li, L.; Zhang, F.; He, G. Bent-Twisted Block Copolymer Anion Exchange Membrane with Improved Conductivity. *J. Memb. Sci.* **2018**, *550* (May 2017), 59–71. https://doi.org/10.1016/j.memsci.2017.12.044.

(29) Pan, Y.; Jiang, K.; Sun, X.; Ma, S.; So, Y. M.; Ma, H.; Yan, X.; Zhang, N.; He, G. Facilitating Ionic Conduction for Anion Exchange Membrane via Employing Star-Shaped

Block Copolymer. *J. Memb. Sci.* **2021**, *630* (February), 119290. https://doi.org/10.1016/j.memsci.2021.119290.

(30) Danks, T. N.; Slade, R. C. T.; Varcoe, J. R. Comparison of PVDF- and FEP-Based Radiation-Grafted Alkaline Anion-Exchange Membranes for Use in Low Temperature Portable DMFCs. *J. Mater. Chem.* **2002**, *12* (12), 3371–3373. https://doi.org/10.1039/b208627a.

(31) Danks, T. N.; Slade, R. C. T.; Varcoe, J. R. Alkaline Anion-Exchange Radiation-Grafted Membranes for Possible Electrochemical Application in Fuel Cells. *J. Mater. Chem.* **2003**, *13* (4), 712–721. https://doi.org/10.1039/b212164f.

(32) Herman, H.; Slade, R. C. T.; Varcoe, J. R. The Radiation-Grafting of Vinylbenzyl Chloride onto Poly(Hexafluoropropylene-Co-Tetrafluoroethylene) Films with Subsequent Conversion to Alkaline Anion-Exchange Membranes: Optimisation of the Experimental Conditions and Characterisation. *J. Memb. Sci.* **2003**, *218* (1–2), 147–163. https://doi.org/10.1016/S0376-7388(03)00167-4.

(33) Page, O. M. M.; Poynton, S. D.; Murphy, S.; Lien Ong, A.; Hillman, D. M.; Hancock, C.

A.; Hale, M. G.; Apperley, D. C.; Varcoe, J. R. The Alkali Stability of Radiation-Grafted Anion-Exchange Membranes Containing Pendent 1-Benzyl-2,3-Dimethylimidazolium Head-Groups. *RSC Adv.* **2013**, *3* (2), 579–587. https://doi.org/10.1039/c2ra22331g.

(34) Savina, I. N.; Galaev, I. Y.; Mattiasson, B. Anion-Exchange Supermacroporous Monolithic Matrices with Grafted Polymer Brushes of N,N-Dimethylaminoethyl-Methacrylate. *J. Chromatogr. A* **2005**, *1092* (2), 199–205. https://doi.org/10.1016/j.chroma.2005.06.094.

(35) Sherazi, T. A.; Yong Sohn, J.; Moo Lee, Y.; Guiver, M. D. Polyethylene-Based Radiation Grafted Anion-Exchange Membranes for Alkaline Fuel Cells. *J. Memb. Sci.* **2013**, *441*, 148–157. https://doi.org/10.1016/j.memsci.2013.03.053.

(36) Slade, R. C. T.; Varcoe, J. R. Investigations of Conductivity in FEP-Based Radiation-Grafted Alkaline Anion-Exchange Membranes. *Solid State Ionics* **2005**, *176* (5–6), 585–597. https://doi.org/10.1016/j.ssi.2004.09.044.

(37) Varcoe, J. R.; Slade, R. C. T. An Electron-Beam-Grafted ETFE Alkaline Anion-Exchange Membrane in Metal-Cation-Free Solid-State Alkaline Fuel Cells. *Electrochem. commun.* **2006**, *8* (5), 839–843. https://doi.org/10.1016/j.elecom.2006.03.027.

(38) Varcoe, J. R.; Slade, R. C. T.; Lam How Yee, E.; Poynton, S. D.; Driscoll, D. J.; Apperley, D. C. Poly(Ethylene-Co-Tetrafluoroethylene)-Derived Radiation-Grafted Anion-Exchange Membrane with Properties Specifically Tailored for Application in Metal-Cation-Free Alkaline Polymer Electrolyte Fuel Cells. *Chem. Mater.* **2007**, *19* (10), 2686–2693. https://doi.org/10.1021/cm062407u.

(39) Li, N.; Yan, T.; Li, Z.; Thurn-Albrecht, T.; Binder, W. H. Comb-Shaped Polymers to Enhance Hydroxide Transport in Anion Exchange Membranes. *Energy Environ. Sci.* **2012**, *5* (7), 7888–7892. https://doi.org/10.1039/c2ee22050d.

(40) He, Y.; Si, J.; Wu, L.; Chen, S.; Zhu, Y.; Pan, J.; Ge, X.; Yang, Z.; Xu, T. Dual-Cation Comb-Shaped Anion Exchange Membranes: Structure, Morphology and Properties. *J. Memb. Sci.* **2016**, *515*, 189–195. https://doi.org/10.1016/j.memsci.2016.05.058.

(41) Singh, G.; Kumar, M.; Thomas, T. S.; Nagaiah, T. C.; Mandal, D. Pendent Persubstituted Imidazolium and a Polyimidazolium Cross-Linked Polymer as Robust Alkaline Anion Exchange Membranes for Solid-State Zn-Air Batteries. *ACS Appl. Energy Mater.* **2021**, *4* (12), 14689–14699. https://doi.org/10.1021/acsaem.1c03318.

(42) Shin, D. W.; Guiver, M. D.; Lee, Y. M. Hydrocarbon-Based Polymer Electrolyte Membranes: Importance of Morphology on Ion Transport and Membrane Stability. *Chem. Rev.* **2017**, *117* (6), 4759–4805. https://doi.org/10.1021/acs.chemrev.6b00586.

(43) Frischknecht, A. L.; In 'T Veld, P. J.; Kolesnichenko, I. V.; Arnot, D. J.; Lambert, T. N. Morphology and Dynamics in Hydroxide-Conducting Polysulfones. *ACS Appl. Polym. Mater.* **2022**, *4* (4), 2470–2480. https://doi.org/10.1021/acsapm.1c01798.

(44) Li, Q.; Liu, L.; Miao, Q.; Jin, B.; Bai, R. Hydroxide-Conducting Polymer Electrolyte Membranes from Aromatic ABA Triblock Copolymers. *Polym. Chem.* **2014**, *5* (7), 2208–2213. https://doi.org/10.1039/c3py01673k.

(45) Price, S. C.; Ren, X.; Jackson, A. C.; Ye, Y.; Elabd, Y. A.; Beyer, F. L. Bicontinuous Alkaline Fuel Cell Membranes from Strongly Self-Segregating Block Copolymers. *Macromolecules* **2013**, *46* (18), 7332–7340. https://doi.org/10.1021/ma400995n.

(46) Kimura, T.; Akiyama, R.; Miyatake, K.; Inukai, J. Phase Separation and Ion Conductivity in the Bulk and at the Surface of Anion Exchange Membranes with Different Ion Exchange Capacities at Different Humidities. *J. Power Sources* **2018**, *375*, 397–403.

https://doi.org/10.1016/j.jpowsour.2017.06.081.

(47) Akiyama, R.; Yokota, N.; Nishino, E.; Asazawa, K.; Miyatake, K. Anion Conductive Aromatic Copolymers from Dimethylaminomethylated Monomers: Synthesis, Properties, and Applications in Alkaline Fuel Cells. *Macromolecules* **2016**, *49* (12), 4480–4489. https://doi.org/10.1021/acs.macromol.6b00408.

(48) Dong, X.; Hou, S.; Mao, H.; Zheng, J.; Zhang, S. Novel Hydrophilic-Hydrophobic Block Copolymer Based on Cardo Poly(Arylene Ether Sulfone)s with Bis-Quaternary Ammonium Moieties for Anion Exchange Membranes. *J. Memb. Sci.* **2016**, *518*, 31–39. https://doi.org/10.1016/j.memsci.2016.06.036.

(49) Han, G. L.; Xu, P. Y.; Zhou, K.; Zhang, Q. G.; Zhu, A. M.; Liu, Q. L. Fluorene-Containing Poly (Arylene Ether Sulfone) Block Copolymers: Synthesis, Characterization and Application. *J. Memb. Sci.* **2014**, *464*, 72–79. https://doi.org/10.1016/j.memsci.2014.03.062.

(50) Lai, A. N.; Wang, L. S.; Lin, C. X.; Zhuo, Y. Z.; Zhang, Q. G.; Zhu, A. M.; Liu, Q. L. Phenolphthalein-Based Poly(Arylene Ether Sulfone Nitrile)s Multiblock Copolymers as

Anion Exchange Membranes for Alkaline Fuel Cells. *ACS Appl. Mater. Interfaces* **2015**, *7* (15), 8284–8292. https://doi.org/10.1021/acsami.5b01475.

(51) Li, L.; Yue, X.; Wu, W.; Yan, W.; Zeng, M.; Zhou, Y.; Liao, S.; Li, X. Multi-Block Copolymers with Fluorene-Containing Hydrophilic Segments Densely Functionalized by Side-Chain Quaternary Ammonium Groups as Anion Exchange Membranes. *RSC Adv.* **2016**, *6* (47), 41453–41464. https://doi.org/10.1039/c6ra04989c.

(52) Li, X.; Tao, J.; Nie, G.; Wang, L.; Li, L.; Liao, S. Cross-Linked Multiblock Copoly(Arylene Ether Sulfone) Ionomer/Nano-ZrO2 Composite Anion Exchange Membranes for Alkaline Fuel Cells. *RSC Adv.* **2014**, *4* (78), 41398–41410. https://doi.org/10.1039/c4ra06519k.

(53) Liu, L.; Ahlfield, J.; Tricker, A.; Chu, D.; Kohl, P. A. Anion Conducting Multiblock Copolymer Membranes with Partial Fluorination and Long Head-Group Tethers. *J. Mater. Chem. A* **2016**, *4* (41), 16233–16244. https://doi.org/10.1039/c6ta06653d.

(54) Miyake, J.; Fukasawa, K.; Watanabe, M.; Miyatake, K. Effect of Ammonium Groups on the Properties and Alkaline Stability of Poly(Arylene Ether)-Based Anion Exchange Membranes. *J. Polym. Sci. Part A Polym. Chem.* **2014**, *52* (3), 383–389.

https://doi.org/10.1002/pola.27011.

(55) Park, D. Y.; Kohl, P. A.; Beckham, H. W. Anion-Conductive Multiblock Aromatic Copolymer Membranes: Structure-Property Relationships. *J. Phys. Chem. C* **2013**, *117* (30), 15468–15477. https://doi.org/10.1021/jp311987v.

(56) Rao, A. H. N.; Kim, H. J.; Nam, S.; Kim, T. H. Cardo Poly(Arylene Ether Sulfone) Block Copolymers with Pendant Imidazolium Side Chains as Novel Anion Exchange Membranes for Direct Methanol Alkaline Fuel Cell. *Polymer (Guildf).* **2013**, *54* (26), 6918–6928. https://doi.org/10.1016/j.polymer.2013.10.052.

(57) Rao, A. H. N.; Nam, S.; Kim, T. H. Crosslinked Poly(Arylene Ether Sulfone) Block Copolymers Containing Pendant Imidazolium Groups as Both Crosslinkage Sites and Hydroxide Conductors for Highly Selective and Stable Membranes. *Int. J. Hydrogen Energy* **2014**, *39* (11), 5919–5930. https://doi.org/10.1016/j.ijhydene.2014.01.191.

(58) Guo, D.; Lai, A. N.; Lin, C. X.; Zhang, Q. G.; Zhu, A. M.; Liu, Q. L. Imidazolium-Functionalized Poly(Arylene Ether Sulfone) Anion-Exchange Membranes Densely Grafted with Flexible Side Chains for Fuel Cells. *ACS Appl. Mater. Interfaces* **2016**, *8* (38), 25279–

25288. https://doi.org/10.1021/acsami.6b07711.

(59) Singh, A. K.; Pandey, R. P.; Shahi, V. K. Fluorenyl Phenolphthalein Groups Containing a Multi-Block Copolymer Membrane for Alkaline Fuel Cells. *RSC Adv.* **2014**, *4*(42), 22186–22193. https://doi.org/10.1039/c4ra01999g.

(60) Zhao, Z.; Wang, J.; Li, S.; Zhang, S. Synthesis of Multi-Block Poly(Arylene Ether Sulfone) Copolymer Membrane with Pendant Quaternary Ammonium Groups for Alkaline Fuel Cell. *J. Power Sources* **2011**, *196* (10), 4445–4450. https://doi.org/10.1016/j.jpowsour.2011.01.081.

(61) Buggy, N. C.; Du, Y.; Kuo, M. C.; Seifert, S.; Gasvoda, R. J.; Agarwal, S.; Coughlin, E. B.; Herring, A. M. Designing Anion-Exchange Ionomers with Oriented Nanoscale Phase Separation at a Silver Interface. *J. Phys. Chem. C* **2021**, *125* (37), 20592–20605. https://doi.org/10.1021/acs.jpcc.1c06036.

(62) Li, X.; Liu, Q.; Yu, Y.; Meng, Y. Synthesis and Properties of Multiblock Ionomers Containing Densely Functionalized Hydrophilic Blocks for Anion Exchange Membranes. *J. Memb. Sci.* **2014**, *467*, 1–12. https://doi.org/10.1016/j.memsci.2014.05.016.

(63) Tanaka, M.; Fukasawa, K.; Nishino, E.; Yamaguchi, S.; Yamada, K.; Tanaka, H.; Bae, B.; Miyatake, K.; Watanabe, M. Anion Conductive Block Poly(Arylene Ether)s: Synthesis, Properties, and Application in Alkaline Fuel Cells. *J. Am. Chem. Soc.* **2011**, *133* (27), 10646–10654. https://doi.org/10.1021/ja204166e.

(64) Weiber, E. A.; Meis, D.; Jannasch, P. Anion Conducting Multiblock Poly(Arylene Ether Sulfone)s Containing Hydrophilic Segments Densely Functionalized with Quaternary Ammonium Groups. *Polym. Chem.* **2015**, *6* (11), 1986–1996. https://doi.org/10.1039/c4py01588f.

(65) Xu, P. Y.; Zhou, K.; Han, G. L.; Zhang, Q. G.; Zhu, A. M.; Liu, Q. L. Effect of Fluorene Groups on the Properties of Multiblock Poly(Arylene Ether Sulfone)s-Based Anion-Exchange Membranes. *ACS Appl. Mater. Interfaces* **2014**, *6* (9), 6776–6785. https://doi.org/10.1021/am5017599.

(66) Yan, J.; Hickner, M. A. Anion Exchange Membranes by Bromination of Benzylmethyl-Containing Poly(Sulfone)S. *Macromolecules* **2010**, *43* (5), 2349–2356. https://doi.org/10.1021/ma902430y.

(67) Vinodh, R.; Atchudan, R.; Kim, H.-J.; Yi, M. Recent Advancements in Polysulfone Based Membranes for Fuel Cell (PEMCs, DMFCs, and AMFCs) Applications: A Critical Review. *Polymers (Basel).* **2022**, *14* (300), 1–22.

(68) Hu, Z.; Tang, W.; Ning, D.; Zhang, X.; Bi, H.; Chen, S. Fluorenyl-Containing Quaternary Ammonium Poly(Arylene Ether Sulfone)s for Anion Exchange Membrane Applications. *Fuel Cells* **2016**, *16* (5), 557–567. https://doi.org/10.1002/fuce.201600015.

(69) Li, X.; Yu, Y.; Liu, Q.; Meng, Y. Synthesis and Properties of Anion Conductive Multiblock Copolymers Containing Tetraphenyl Methane Moieties for Fuel Cell Application. *J. Memb. Sci.* **2013**, *436*, 202–212. https://doi.org/10.1016/j.memsci.2013.02.041.

(70) Mayadevi, T. S.; Sung, S.; Chae, J. E.; Kim, H. J.; Kim, T. H. Quaternary Ammonium-Functionalized Poly(Ether Sulfone Ketone) Anion Exchange Membranes: The Effect of Block Ratios. *Int. J. Hydrogen Energy* **2019**, *44* (33), 18403–18414. https://doi.org/10.1016/j.ijhydene.2019.05.061.

(71) Sung, S.; T.S., M.; Chae, J. E.; Kim, H. J.; Kim, T. H. Effect of Increasing Hydrophilic–Hydrophobic Block Length in Quaternary Ammonium-Functionalized Poly(Ether Sulfone)

Block Copolymer for Anion Exchange Membrane Fuel Cells. *J. Ind. Eng. Chem.* **2020**, *81*, 124–134. https://doi.org/10.1016/j.jiec.2019.08.062.

(72) Liu, Y.; Horan, J. L.; Schlichting, G. J.; Caire, B. R.; Liberatore, M. W.; Hamrock, S. J.; Haugen, G. M.; Yandrasits, M. A.; Seifert, S.; Herring, A. M. A Small-Angle X-Ray Scattering Study of the Development of Morphology in Films Formed from the 3M Perfluorinated Sulfonic Acid Ionomer. *Macromolecules* **2012**, *45* (18), 7495–7503. https://doi.org/10.1021/ma300926e.

(73) Schlichting, G. J.; Horan, J. L.; Jessop, J. D.; Nelson, S. E.; Seifert, S.; Yang, Y.; Herring, A. M. A Hybrid Organic/Inorganic Ionomer from the Copolymerization of Vinylphosphonic Acid and Zirconium Vinylphosphonate. *Macromolecules* **2012**, *45* (9), 3874–3882. https://doi.org/10.1021/ma300196y.

(74) Li, Y.; Jackson, A. C.; Beyer, F. L.; Knauss, D. M. Poly(2,6-Dimethyl-1,4-Phenylene Oxide) Blended with Poly(Vinylbenzyl Chloride)- b -Polystyrene for the Formation of Anion Exchange Membranes. *Macromolecules* **2014**, *47* (19), 6757–6767. https://doi.org/10.1021/ma500993s.

(75) Hickner, M. A.; Herring, A. M.; Coughlin, E. B. Anion Exchange Membranes: Current Status and Moving Forward. *J. Polym. Sci. Part B Polym. Phys.* **2013**, *51* (24), 1727–1735. https://doi.org/10.1002/polb.23395.

(76) Zhang, H. W.; Chen, D. Z.; Xianze, Y.; Yin, S. B. Anion-Exchange Membranes for Fuel Cells: Synthesis Strategies, Properties and Perspectives. *Fuel Cells* **2015**, *15* (6), 761–780. https://doi.org/10.1002/fuce.201500039.

(77) Clouet, G.; Juhl, H. J. Free Radical Synthesis of α,Ω-primary Amino Functionalized Polyisoprene through the Functional Thermal Inferter [Bis(N-(2-phthalimidoethyl)Piperazine)]Thiuram Disulfide. *Macromol. Chem. Phys.* **1994**, *195* (1), 243–251. https://doi.org/10.1002/macp.1994.021950122.

(78) Pryor, W. A.; Pickering, T. L. Reactions of Radicals. Rates of Chain Transfer of Disulfides and Peroxides with the Polystyryl Radical. *J. Am. Chem. Soc.* **1962**, *84* (14), 2705–2711. https://doi.org/10.1021/ja00873a012.

(79) Tobolsky, A. V.; Baysal, B. The Reaction between Styrene and Ring Disulfides: Copolymerization Effected by the Chain Transfer Reaction. *J. Am. Chem. Soc.* **1953**, *75*,

1757.

(80) Tirelli, N.; Hunkeler, D. J. Variations in the Diallyldimethylammonium Chloride (DADMAC) Polymers Architectures: PEG/DADMAC Blocks and Partially Quaternarized Polymers. *Macromol. Chem. Phys.* **1999**, *200* (5), 1068–1073. https://doi.org/10.1002/(SICI)1521-3935(19990501)200:5<1068::AID-MACP1068>3.0.CO;2-0.

(81) Assem, Y.; Greiner, A.; Agarwal, S. Microwave-Assisted Controlled Ring-Closing Cyclopolymerization of Diallyldimethylammonium Chloride Via the RAFT Process. *Macromol. Rapid Commun.* **2007**, *28*, 1923–1928. https://doi.org/10.1002/marc.200700377.

(82) Wang, J.; Zhao, Z.; Gong, F.; Li, S.; Zhang, S. Synthesis of Soluble Poly(Arylene Ether Sulfone) Ionomers with Pendant Quaternary Ammonium Groups for Anion Exchange Membranes. *Macromolecules* **2009**, *42* (22), 8711–8717. https://doi.org/10.1021/ma901606z.

(83) Sarode, H. N.; Yang, Y.; Motz, A. R.; Li, Y.; Knauss, D. M.; Seifert, S.; Herring, A. M.

Understanding Anion, Water, and Methanol Transport in a Polyethylene-b-Poly(Vinylbenzyl Trimethylammonium) Copolymer Anion-Exchange Membrane for Electrochemical Applications. *J. Phys. Chem. C* **2017**, *121* (4), 2035–2045. https://doi.org/10.1021/acs.jpcc.6b09205.

(84) Choi, J. H.; Ye, Y.; Elabd, Y. A.; Winey, K. I. Network Structure and Strong Microphase Separation for High Ion Conductivity in Polymerized Ionic Liquid Block Copolymers. *Macromolecules* **2013**, *46* (13), 5290–5300. https://doi.org/10.1021/ma400562a.

(85) Cotanda, P.; Sudre, G.; Modestino, M. A.; Chen, X. C.; Balsara, N. P. High Anion Conductivity and Low Water Uptake of Phosphonium Containing Diblock Copolymer Membranes. *Macromolecules* **2014**, *47* (21), 7540–7547. https://doi.org/10.1021/ma501744w.